Detection of Neovascularization Near the Optic Disk Due to Diabetic Retinopathy

Diego F. G. Coelho*, Rangaraj M. Rangayyan*, Vassil S. Dimitrov*‡
*Department of Electrical and Computer Engineering, University of Calgary, Calgary, Alberta, Canada.
‡Computer Modelling Group, Ltd., Calgary, Alberta, Canada.

***Abstract*—We propose a technique for detection of neovascularization near the optic disk due to diabetic retinopathy. Images of the retinal fundus are analyzed using a measure of angular spread of the Fourier power spectrum of the gradient magnitude of the original images using the horizontal and vertical Prewitt operators. The entropy of the angular spread of the Fourier power spectrum and spatial variance are adopted to distinguish normal optic disks from those affected by neovascularization. The two-sided Kolmogorov–Smirnov nonparametric test is used to evaluate the significance of the difference of entropy between normal and abnormal optic disks. Based on the computed measures, we employ a linear classifier to discriminate normal from abnormal optic disks. The proposed method was able to classify a small set of five normal and five neovascularization cases with 100% accuracy.**

***Index Terms*—Retinal Image Analysis, Fourier Spectral Analysis, Neovascularization.**

I. Introduction

A. Diabetic Retinopathy

Diabetes can cause retinopathy, referred to as diabetic retinopathy [1]. Diabetic retinopathy includes damage to retinal blood vessels. Diabetic retinopathy is classified into two major groups: proliferative (PDR) and nonproliferative diabetic retinopathy (NPDR).

Signs of NPDR include microaneurysms, intraretinal hemorrhages, and microvascular abnormalities [1]. PDR includes the phenomenon of neovascularization near the optic disk, abbreviated as NVD, or elsewhere in the retina (NVE) [1]. The chances of development of diabetic retinopathy are strongly correlated with factors such as the duration of diabetes and the degree of hyperglycemia [1]. Diabetic retinopathy has been identified as one of the main preventable causes of blindness [1], [2].

B. Computer-aided Diagnosis of Diabetic Retinopathy

Diabetic retinopathy has attracted the attention of the research community involved in biomedical image processing [3], [4]. Several methods have been proposed to detect different aspects of diabetic retinopathy, such as microaneurysms [5], [6]; retinal vascular abnormalities [7], [8]; hemorrhage [9]; and tortuosity [10], [11].

C. Related Works

Mudigonda *et al.* [12] proposed fractal analysis based on box counting for detection of NVD using fundus images. Fractal analysis was performed after preprocessing with Gabors filters to highlight retinal blood vessels.

Daxer [13] employed fractal analysis by means of a density-density correlation function. After determining a threshold value for the fractal dimension, Daxer showed that high values of fractal dimension indicate the existence of PDR.

Lee *et al.* [14] proposed a method for automatic detection of blood vessels for grading the severity of diabetic retinopathy. The method is based on statistical texture analysis, high-order spectrum analysis, and fractal analysis.

Akram *et al.* [15] proposed a method to extract vascular patterns after enhancing the blood vessels using wavelet modeling. They employed statistical classifiers based on the Gaussian mixture model for the detection of neovascularization with high accuracy up to 95%.

Oloumi *et al.* [16] proposed the use of blood vessel thickness for diagnosis of plus disease. They employed Gabor filters to extract the skeleton of the major temporal arcade in retinal fundus images of preterm infants, and achieved an area under the receiver operating characteristic curve of 0.76. This procedure may be applied to analyze vascular dilation due to diabetic retinopathy as well.

D. Scope and Organization of the Present Paper

In this paper, we propose a measure of angular spread of the Fourier power spectrum for the detection of NVD. A portion of a retinal fundus image may be classified into four groups: NVD, NVE, non-optic-disk region of the retina (NOR), and normal optic disk (NOD). In this paper, we concentrate on the discrimination of NVD versus NOD.

Section II provides description of the material and methods used in the present work. Section III presents the results obtained. In Section IV, we propose a scheme for discrimination among the four cases mentioned

978-0-9928-6265-7/16/$31.00 ©2016 IEEE

above. In Section V, we draw conclusions and provide comments on future work.

II. Material and Methods

A. Retinal Fundus Images

The images used in this work were obtained from the MESSIDOR database [17] and are the same as those used by Mudigonda *et al.* [12].

The data set used in the present work includes all five cases of NVD that could be identified and five cases of NOD as normal control cases. We perform image analysis block by block using a window of size 256×256 pixels. The original images are of size 1488×2440 pixels. Zero-valued pixels were appended and the images were reformatted to the size of 1536×2304 pixels. The green channels of the original color images were used. All the computations and analysis were performed with Matlab®.

B. Angular Spread of the Fourier Power Spectrum

Let the given image $f(m,n)$ be represented as a real-valued square matrix of size $N \times N$. First, the gradient magnitude of $f(m,n)$ is obtained using the horizontal and vertical Prewitt operators [18]. In order to reduce artifacts in the Fourier domain due to truncation, the von Hann window [19] is applied. The Fourier power spectrum $|F_s(k,l)|^2$ is obtained in Cartesian representation, converted to polar representation, and denoted as $S(r,\theta)$ [18], [20]. When there is no pixel at the position $[r\cos(\theta), r\sin(\theta)]$, we use quadratic interpolation [21]. The origin with frequency values $(0,0)$ is adopted as the center. The angle θ is evaluated at $0°, 1°, \ldots, 179°$. In this work, we use only matrices of even size and $r = 0, 1, \ldots, N/2-1$. The angular spread of a Fourier power spectrum is defined as

$$S_{a,b}(\theta) = \sum_{r=a}^{b} S(r,\theta), \tag{1}$$

where a and b are nonnegative integers smaller than $N/2$.

In order to perform discrimination between NVD and NOD, we need a measure of the angular spread of the Fourier power spectrum. The entropy of angular spread of a Fourier power spectrum is obtained as

$$H_\theta = -\frac{1}{S}\sum_{\theta} S_{a,b}(\theta)\log_2\left(\frac{S_{a,b}(\theta)}{S}\right), \tag{2}$$

measured in bits of information per polar spectrum component, where S is the normalizing factor given by $S = \sum_\theta S_{a,b}(\theta)$. Due to the presence of randomly oriented patterns of new blood vessels, regions related to NVD are expected to have a broader angular spread of Fourier power spectrum and hence higher H_θ than NOD regions.

Because the spectral components may not be statistically independent due to interpolation, the entropy value obtained as above may be considered as a limiting value.

In addition to H_θ, we use a measure of spatial variance of the original image $f(m,n)$ as

$$\sigma_f^2 = \frac{1}{N^2}\sum_{m=0}^{N-1}\sum_{n=0}^{N-1}\left[f(m,n)-\mu_f\right]^2, \tag{3}$$

where μ_f is the mean value of $f(m,n)$ [18], [20].

Figure 1 shows regions of retinal fundus images presenting the two situations in which we are interested: NOD and NVD. From information theory, we know that the entropy of a given probability density function (PDF) is at its maximum when it is uniform [18]. Also, we know that when a PDF presents a few values with high probability and others with small probability, the entropy is drastically reduced. Therefore, if the angular spread of a Fourier power spectrum does not show a defined direction or a few preferred directions, its entropy will be high and can be an indicative of neovascularization.

We employed an *ad-hoc* technique to select the appropriate interval $[a,b]$ that causes $S_{a,b}(\theta)$ as in (1) to show noticeable difference between the two groups of NOD and NVD. We determined the range $[a,b] = [13, 115]$, which corresponds to normalized radial frequency in the interval $[0.05, 0.45]$. The fraction of energy of the Fourier power spectrum considered for the computation of entropy is shown enclosed between the circles in Figures 1(c) and 1(d).

III. Results

Figure 2 shows the box-plot for the entropy measures for all of the images used in this study. The entropy measures were analyzed using the two-sided Kolmogorov–Smirnov test [22]. The null hypothesis is that the groups NOD and NVD do not present a significant difference in the entropy measures of angular spread of the Fourier power spectrum. Table I shows the p-value and the statistic $D_{\max}$ [22]. The result shows that we do not have the confidence to accept the null hypothesis at the significance level of 5%.

Discrimination between the NVD and NOD groups was done using linear statistical classifiers [23], [24]. We employed the entropy of angular spread of the Fourier power spectrum and spatial variance as discriminant measures, and obtained 100% correct separation as depicted in Figure 3. Table II shows the parameter values for the classifier in Figure 3. Due to 100% correct separation, the resubstitution error is zero and the model

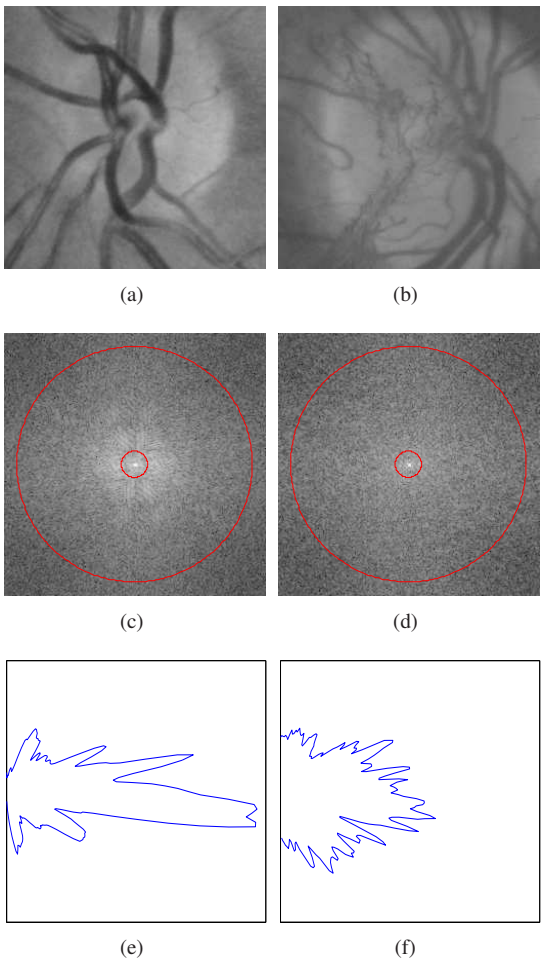

Figure 1. (a) and (b) show image regions presenting cases of NOD and NVD, respectively. (c) and (d) show the log-magnitude of the Fourier power spectra of the gradient magnitude of (a) and (b) using the horizontal and vertical Prewitt operators. (e) and (f) show the plot of angular spread of the Fourier power spectra of the gradient magnitude of (a) and (b) using the horizontal and vertical Prewitt operators. The angles in (e) and (f) agree with the orientation in (c) and (d) but are displaced by $-90°$ with respect to the orientation in (a) and (b).

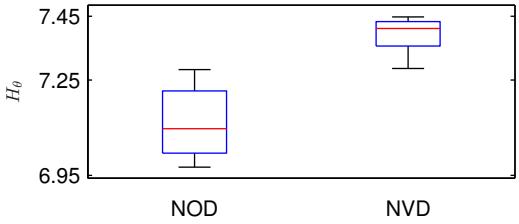

Figure 2. Box-plot for the entropy of angular spread of the Fourier power spectrum for five images of NOD and five images of NVD.

Table I
THE RESULTS OF THE TWO-SIDED KOLMOGOROV–SMIRNOV TEST FOR COMPARISON BETWEEN THE ENTROPY MEASURES FOR NOD VERSUS NVD

Test	p-value	Statistic
Kolmogorov–Smirnov	3.80×10^{-2}	$D_{\max} = 1.00$

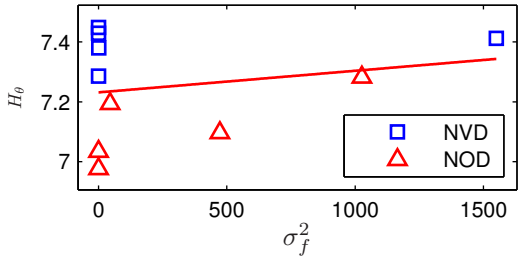

Figure 3. Linear classifier for discrimination of NOD versus NVD based on spatial variance and entropy of angular spread of the Fourier power spectrum.

loss [24] is low (0.20), which confirm the effectiveness of the classifier.

IV. PROCEDURE FOR DISCRIMINATION BETWEEN NVD AND NOD

In general, images from screening programs and clinical studies could contain regions of the four types: NOD, NOR, NVD, and NVE. Thus, we need a procedure to classify image regions among the four groups. For this purpose, we could first detect the optic-disk region with the method of Rangayyan *et al.* [25] using Gabor filters and phase portrait analysis. Then, we can split a given fundus image into two parts, one containing the optic disk and the other containing the remaining image. With the portions of images containing the optic disk, we can perform discrimination between NOD and NVD using the methods presented in Section III. With the remaining portions of the images, we can employ the same procedure modified to discriminate between NOR and NVE. In this manner, we can detect neovascularization, whether it occurs near the optic disk or elsewhere in the retina. Figure 4 shows a block diagram of this procedure, which is being developed.

Table II
PARAMETERS OF THE LINEAR CLASSIFIER FOR DISCRIMINATION OF NOD VERSUS NVD

$a\sigma_f^2 + bH_\theta + c$	$0.003\sigma_f^2 - 35.184H_\theta + 254.431$

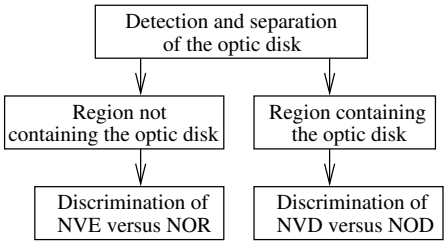

Figure 4. Block diagram for discrimination among the four groups NOD, NOR, NVD, and NVE using a method to detect the optic disk.

V. Conclusion and Future Work

We have proposed the use of a measure of the angular spread of the Fourier power spectra of retinal fundus images for detection of regions of NVD due to diabetic retinopathy. It was shown that the NVD and NOD groups present different angular spread of the Fourier power spectrum. The obtained measures were statistically analyzed using the two-sided Kolmogorov–Smirnov test and shown to be significantly different. A linear classifier provided 100% accuracy with a small set of ten images.

Future work will include the application of the proposed method to images containing NVE, testing with a larger data set, cross-validation of the results of pattern classification, and comparative analysis with other related reports. More advanced work may include the use of the proposed procedure incorporating detection of the optic disk and identification of NVD and NVE.

Acknowledgments

This project was supported by the Natural Sciences and Engineering Research Council of Canada (NSERC). We thank Faraz Oloumi for his assistance in this work.

References

[1] J. Noble and V. Chaudhary, "Diabetic retinopathy," *Canadian Medical Association Journal*, vol. 182, no. 15, pp. 1646–1646, 2010.

[2] D. S. Fong, L. Aiello, T. W. Gardner, G. L. King, G. Blankenship, J. D. Cavallerano, F. L. Ferris, and R. Klein, "Retinopathy in diabetes," *Diabetes Care*, vol. 27, no. suppl 1, pp. s84–s87, 2004.

[3] A. Ahmad, A. B. Mansoor, R. Mumtaz, M. Khan, and S. H. Mirza, "Image processing and classification in diabetic retinopathy: A review," in *5th European Workshop on Visual Information Processing (EUVIP)*. Paris, Ile-de-France, France: IEEE, 2014, pp. 1–6.

[4] M. A. Rao, D. Lamani, R. Bhandarkar, and T. C. Manjunath, "Automated detection of diabetic retinopathy through image feature extraction," in *International Conference on Advances in Electronics, Computers and Communications (ICAECC)*. Bangalore, Karnataka, India: IEEE, 2014, pp. 1–6.

[5] A. Agrawal, C. Bhatnagar, and A. S. Jalal, "A survey on automated microaneurysm detection in diabetic retinopathy retinal images," in *International Conference on Information Systems and Computer Networks (ISCON)*. Chaumuhan, Uttar Pradesh, India: IEEE, 2013, pp. 24–29.

[6] M. Niemeijer, B. van Ginneken, M. J. Cree, A. Mizutani, G. Quellec, C. I. Sanchez, B. Zhang, R. Hornero, M. Lamard, C. Muramatsu, X. Wu, G. Cazuguel, J. You, A. Mayo, Q. Li, Y. Hatanaka, B. Cochener, C. Roux, F. Karray, M. Garcia, H. Fujita, and M. D. Abramoff, "Retinopathy online challenge: Automatic detection of microaneurysms in digital color fundus photographs," *IEEE Transactions on Medical Imaging*, vol. 29, no. 1, pp. 185–195, 2010.

[7] V. Joshi, C. Agurto, R. VanNess, S. Nemeth, P. Soliz, and S. Barriga, "Comprehensive automatic assessment of retinal vascular abnormalities for computer-assisted retinopathy grading," in *36th Annual International Conference of the IEEE Engineering in Medicine and Biology Society (EMBC)*. Chicago, Illinois, USA: IEEE, 2014, pp. 6320–6323.

[8] F. Oloumi, R. M. Rangayyan, and A. L. Ells, "Computer-aided diagnosis of proliferative diabetic retinopathy via modeling of the major temporal arcade in retinal fundus images," *Journal of Digital Imaging*, vol. 26, no. 6, pp. 1124–1130, Dec. 2013.

[9] D. Zhang, X. Li, X. Shang, Y. Yi, and Y. Wang, "Robust hemorrhage detection in diabetic retinopathy image," in *First Asian Conference on Pattern Recognition (ACPR)*. Beijing, China: IEEE, 2011, pp. 209–213.

[10] E. Poletti, E. Grisan, and A. Ruggeri, "Image-level tortuosity estimation in wide-field retinal images from infants with retinopathy of prematurity," in *Annual International Conference of the IEEE Engineering in Medicine and Biology Society (EMBC)*. San Diego, California, USA: IEEE, 2012, pp. 4958–4961.

[11] F. Oloumi, R. M. Rangayyan, and A. L. Ells, "Computer-aided diagnosis of plus disease in retinal fundus images of preterm infants via measurement of vessel tortuosity," in *37th Annual International Conference of the IEEE Engineering in Medicine and Biology Society (EMBC)*. Milan, Lombardy, Italy: IEEE, 2015, pp. 4338–4342.

[12] S. Mudigonda, F. Oloumi, K. M. Katta, and R. M. Rangayyan, "Fractal analysis of neovascularization due to diabetic retinopathy in retinal fundus images," in *The 5th IEEE International Conference on E-Health and Bioengineering - EHB*. Iaşi, Romania: IEEE, Nov. 2015.

[13] A. Daxer, "The fractal geometry of proliferative diabetic retinopathy: implications for the diagnosis and the process of retinal vasculogenesis," *Current Eye Research*, vol. 12, no. 12, pp. 1103–1109, 1993.

[14] J. Lee, B. C. Y. Zee, and Q. Li, "Detection of neovascularization based on fractal and texture analysis with interaction effects in diabetic retinopathy," *PLoS ONE*, vol. 8, no. 12, p. e75699, Dec. 2013.

[15] M. U. Akram, A. Tariq, and S. Khan, "Detection of neovascularization for screening of proliferative diabetic retinopathy," in *Image Analysis and Recognition*, ser. Lecture Notes in Computer Science, A. Campilho and M. Kamel, Eds. Springer, 2012, vol. 7325, pp. 372–379.

[16] F. Oloumi, R. M. Rangayyan, P. Casti, and A. L. Ells, "Computer-aided diagnosis of plus disease via measurement of vessel thickness in retinal fundus images of preterm infants," *Computers in Biology and Medicine*, vol. 66, pp. 316–329, 2015.

[17] E. Decencière, X. Zhang, G. Cazuguel, B. Lay, B. Cochener, C. Trone, P. Gain, R. Ordonez, P. Massin, A. Erginay, B. Charton, and J.-C. Klein, "Feedback on a publicly distributed image database: The MESSIDOR database," *Image Analysis & Stereology*, vol. 33, no. 3, pp. 231–234, 2014.

[18] A. K. Jain, *Fundamentals of Digital Image Processing*. Prentice Hall Information and System Sciences Series, 1989.

[19] A. V. Oppenheim, R. W. Schafer, M. T. Yoder, and W. T. Padgett, *Discrete Time Signal Processing*, 3rd ed. Prentice-Hall, Inc., 2009.

[20] R. M. Rangayyan, *Biomedical Image Analysis*. CRC Press, 2005.

[21] N. A. Dodgson, "Quadratic interpolation for image resampling,"

IEEE Transactions on Image Processing, vol. 6, no. 9, pp. 1322–1326, 1997.

[22] G. Casella and R. L. Berger, *Statistical Inference*, 2nd ed. Duxbury Advanced Series, 2002.

[23] R. Herbrich, *Learning Kernel Classifiers: Theory and Algorithms*. MIT Press, 2001.

[24] R. O. Duda, P. E. Hart, and D. G. Stork, *Pattern Classification*. John Wiley & Sons, Inc., 1997.

[25] R. M. Rangayyan, X. Zhu, F. J. Ayres, and A. L. Ells, "Detection of the optic nerve head in fundus images of the retina with Gabor filters and phase portrait analysis," *Journal of Digital Imaging*, vol. 23, no. 4, pp. 438–453, Aug. 2010.